

FINAL REPORT on
NASA-Ames Cooperative Agreement NCC 2-364

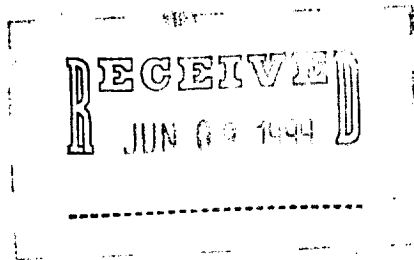
EVOLUTION OF PHOTON AND PARTICLE SPECTRA IN
COMPACT, LUMINOUS OBJECTS

performed by
the New Mexico Institute of Mining and Technology
Socorro, NM 87801

Principal Investigator:
Jean A. Eilek, New Mexico Tech

Co-investigator:
Lawrence J. Caroff, NASA-Ames Research Center

period covered:
September 1990 - August 1995



Rec'd.
JUN 08 1994
cc 2024-3 ✓
CASI

ABSTRACT

Physical conditions in the radiating plasma in the cores of radio-strong quasars and active galactic nuclei cannot be derived from observations until the effects of relativistic aberration are understood. This requires determining both the bulk flow speeds and any wave or signal speed in the parsec-scale nuclear jets. In this project we studied several aspects of such waves.

We considered constraints on jet deceleration by mass pickup, and found that bolometric luminosities of the active nuclei cannot constrain core jet speeds usefully. We also simulated observations of ballistic, helical trajectories and helical waves moving directly outwards along the jet. We found that ballistic trajectories are not allowed by the data; the helical features seen are very likely to be helical waves.

We believe these are waves propagating in the jet plasma. To this end, we studied waves propagating in relativistic pair plasma jets. In particular, we undertook a program whose goal was to determine the nature of waves which can propagate in relativistic pair plasmas, and how such waves propagating in streaming jet plasma would be observed by an external observer. We developed the possibility of using pulsars as test cases for our models; this takes advantage of new technology in pulsar observations, and the similarity of the physical conditions in the pulsar magnetosphere to the dense, relativistic pair plasmas which exist in radio-strong quasars.

PROJECT DESCRIPTION

The nuclear plasma in radio-strong quasars and active nuclei is probably dominated by relativistic electrons and positrons, and is also likely to be strongly magnetized. We have suggested previously that an important distinction between radio-strong and radio-weak objects is the strength of the nuclear magnetic field. Strong fields can confine and accelerate the plasma into a relativistic jet outflow; in addition strong fields lead to rapid radiative energy losses, so that *in situ* acceleration of the particles must be taking place. Thus, our previous results on thermalization of the pair-photon spectra are likely to be dramatically changed in the strong-field situation.

In order to extend our previous work to the strong-field case, basic parameters (such as density and pressure) of the nuclear plasma must be estimated. In the non-magnetized case, where there is no compelling reason to introduce relativistic beaming or strong anisotropy, the observed photon spectra and inferred sizes can be interpreted straightforwardly in terms of these basic plasma parameters. However, emission from the radio-strong sources is likely to be highly anisotropic, due to directed relativistic motion of the emitting plasma. We must understand the nature of the flow, and its effect on observed emission, in order to interpret the observations in terms of these same basic parameters. We do not believe the nature of the flow is well understood; but new VLB images of pc-scale jets (PSJ) in radio-strong sources will make possible a more detailed study of this flow field than had been justified before.

Most previous models of these jets assumed the jets contained a uniform plasma flow, at some speed $v_b = \beta_b c$ (with associated Lorentz factor γ_b ; for instance, Königl 1981). An observer at an angle θ to the flow sees the comoving flux density enhanced by a factor $\delta^{(2+\alpha)}$ if $\delta(\theta) = [\gamma_b(1 - \beta_b \cos \theta)]^{-1}$ and α is the spectral index of the radiation. (For unresolved features, this becomes $\delta^{(3+\alpha)}$). This can lead to a strong enhancement of the emission, for small angles and high speeds (“Doppler boosting”). In addition, observed jets are not uniform, but rather have bright “knots”, which have been modelled as shocks moving at some unspecified speed relative to the flow (for instance, Hughes *et al.* 1985, Marscher and Gear 1985). If the net speed of the feature is v_s , the same observer sees an apparent transverse motion of the feature, $v_{app} = \beta_s \sin \theta / [1 - \beta_s \cos \theta]$. For $\theta \ll 1$ and $\gamma_s \gg 1$, $\beta_{app} > 1$ is possible; this is “superluminal motion”.

These simple models have had good success in describing distributions of apparent velocities, and in predicting Compton-scattered X-ray and γ -ray fluxes from radio-strong nuclei. However, recent VLB images (for instance, Wilkinson *et al.* 1990; Readhead *et al.* 1990) show more complex structure; the evidence now is that the emission comes from *helical* features which seem to lie close to the jet surface. Thus, the flows are not uniform, nor do simple shocks seem able to describe the features. Some authors have suggested the helical tracks are ballistic trajectories; to us they suggest helical waves propagating along the jet, at some β_w, γ_w relative to the jet plasma. The possibility of waves is important, as the Doppler boosting factor ($\sim \gamma_b$) and the apparent velocity factor ($\sim \gamma_b \gamma_w$) are no longer the same. One aspect of the work described in this Report involved testing these two different pictures; we found that helical waves are

In addition, if the flows are nonuniform, we might also wonder if they really maintain a constant flow speed. Both acceleration (in a wind-like regime) and deceleration (due to mass pickup) are possible in principle; one might expect initial acceleration, out to some point where mass pickup dominates and the flow slows down. One aspect of this question involves how the pc-scale jets connect to the larger, kpc-scale jets (KSJ) which also exist in these objects. There are several indirect arguments which suggest the large-scale jets are moving subrelativistically; some authors have suggested such deceleration would dump large amounts of kinetic energy into the surrounding medium, which would be detectable.

Our work during the period which this Report covers addressed some basic aspects of possible flow fields and wave motions in the PSJs, and their consequences for observations. We studied ways in which existing observations can be used to determine the flow speed (which is critical in connecting observed luminosity to comoving densities and energies). In particular, we studied the nature of wave motion in relativistic jet plasmas. Electrodynamical models of the origin of the jet (Lovelace, Wang & Sulkanen 1987; Wang, Sulkanen & Solvelace 1990), in addition to our previous work on weak-field nuclei, strongly suggest the jet material is a pair plasma, at least on parsec scales. To gain insight, we exploited the similarity of this environment to that in pulsar polar caps. The pulsar situation is probably more extreme than in PSJ's, but it has also been better studied, and we therefore developed results and techniques for the pulsar problem which we anticipate can also be used for the PSJ problem.

I. DECELERATING RELATIVISTIC PC-SCALE JETS

The goal of this part of the work was to determine whether simple energetic considerations, used in conjunction with observations of active nuclei, can constrain the bulk flow speed in PSJ. In particular, superluminal PSJ generally connect to larger-scale KSJ. Simple models of the PSJ assume relativistic bulk flow speeds, as discussed above. However, several arguments suggest that flow speeds in the KSJ are subluminal: the two-sidedness of the KSJ, the bends and wiggles seen in some, and the detection of subluminal proper

motion of features in M87 (Biretta *et al.* 1989) all suggest that flow speeds are $\ll c$ in \gtrsim kpc scales. If both inferences are correct, then the jets must decelerate between pc and kpc scales. They probably do this by mass pickup, which conserves momentum flux (climbing out of the galaxy's potential well will provide only a small momentum flux change, and can be ignored to first order). In this case, the jets must lose kinetic energy in the deceleration; several authors have suggested that this "lost" kinetic energy would be absorbed by the ambient medium, and be observable (or, in fact, violate observable limits) in other frequency bands.

We used basic energetics to investigate this idea. We anticipated that this work might provide constraints on the bulk γ_b in the jets, which would constrain the contribution of the γ_b to the superluminal signal speed, and thus require large wave speeds. However, we found that the constraints are not very severe; $\gamma_b \gg 1$ cannot be ruled out.

The analysis starts with general expressions for mass, momentum and energy fluxes in a jet with cross-section A , density ρ , pressure p , and speed $v = \beta c$ (for instance, Weinberg 1972, or Landau and Lifshitz 1959). The mass flux through A is

$$S = \gamma \rho c A ; \quad (1)$$

the momentum flux is

$$\Pi = \gamma^2 \beta^2 A \left(\rho c^2 + \frac{\Gamma}{\Gamma - 1} p \right) \quad (2)$$

and the "usable" energy flux (omitting a ρc^2 term) is

$$L = \gamma \beta c A \left[(\gamma - 1) \rho c^2 + \frac{\Gamma}{\Gamma - 1} \gamma p \right] \quad (3)$$

If gravitational effects are small (which will hold if the jet plasma is internally relativistic in the core), deceleration will take place at constant momentum flux. If we label the core jet by "c" and the kpc-scale jet by "j", the mass flux ratio will be

$$\frac{S_j}{S_c} = \frac{\gamma_c \beta_c (1 + e_c)}{\gamma_j \beta_j (1 + e_j)} \quad (4)$$

where we have defined

$$e = \frac{\Gamma}{\Gamma - 1} \frac{p}{\rho c^2}.$$

The energy flux ratio will be

$$\frac{L_j}{L_c} = \frac{\beta_c}{\beta_j} \frac{(1 + e_j - 1/\gamma_j)}{(1 + e_j)} \frac{(1 + e_c)}{(1 + e_c - 1/\gamma_c)} \quad (5)$$

These relations were investigated algebraically and numerically. We gain the most insight by considering the limit of a relativistic core jet: $\beta_c \rightarrow 1$, $\gamma_c \gg 1$. Then, (5) simplifies to

$$\frac{L_j}{L_c} \simeq \frac{\beta_c}{\beta_j} \frac{(1 + e_j - 1/\gamma_j)}{(1 + e_j)} \quad (6)$$

Two conclusions follow directly. First, if the KSJ is *cold* (that is, $e_j \ll 1$) and slow ($\beta_j \ll 1$), then $L_j/L_c \simeq \beta_j/2$ and, indeed, nearly all of the energy flux is “lost” from the jet. However, if the KSJ is a bit warm, this need not be the case: $L_j = L_c$ if the internal energy of the KSJ satisfies

$$1 + e_j = \left(\frac{1 + \beta_j}{1 - \beta_j} \right)^{1/2} \simeq 1 + \beta_j \quad (7)$$

This condition is only a very weak constraint on the KSJ; an internally warm jet can account for all of the “lost” kinetic energy, and can also be consistent with observational constraints on KSJ. The reason this condition is not more severe, is the large amount of mass that must be entrained to decelerate the jet. In the same limit of a relativistic core jet, a slow KSJ and the internal energy from (7), (4) becomes

$$\frac{S_j}{S_c} = \frac{\gamma_c(1 + e_c)}{\beta_j} \quad (8)$$

which can be quite large; $S_j \gg S_c$, and the “lost” kinetic energy is distributed over a much larger number of particles, keeping e_j low.

Thus, this analysis found that slow speeds, $\beta_j \ll 1$, in KSJ do not put any severe constraints on core jet bulk flow speeds: $\gamma_c \gg 1$ is consistent with energetics and bolometric observations of active nuclei. Further analysis will be needed to determine if the high entrainment rate in (8) can actually be met in real galaxies.

To summarize: we found that the constraints on jet deceleration are not very severe. If the KSJ is cold (that is, $p_j \ll \rho_j c^2$), then the energy fluxes at PSJ and KSJ scales are related by $L_j/L_c \simeq \beta_j/2$. In this limit most of the kinetic energy of the PSJ is indeed “lost”; presumably it has been dumped into the local ISM, which must reradiate it in some other band. This extra luminosity from the core region should be detectable; thus, decelerated PSJ’s cannot connect with cold KSJ’s. On the other hand, if the KSJ is “warm” (needing only $p_j/\rho_j c^2 \simeq \beta_j$ for β_j subrelativistic), the KSJ energy flux satisfies $L_j \simeq L_c$. Thus, relativistic PSJ’s *can* connect to *warm* KSJ’s; there is no lost energy to be reradiated from the nuclear ISM.

II. SIGNATURES OF HELICAL TRAJECTORIES AND HELICAL WAVES

The goal of this part of the work was to determine the observable signatures of different velocity and magnetic field configurations. In particular we concentrated on ballistic, helical trajectories and on helical waves. Helical trajectories include significant velocity components around the jet as well as along the jet; we also assume the magnetic field follows the helical pattern. Helical waves can have significant transverse magnetic field components, but are assumed to move directly out along the jet, without significant “rotation”.

We address three observable quantities: the synchrotron surface brightness, the linear polarization of the radiation, and the apparent velocity in the plane of the sky. These quantities are measurable with current techniques (for instance, Cawthorne 1991). The surface brightness tends to be slightly limb brightened, and to show helical patterns; the jets are close to symmetric about their center line. VLB polarization has only been measured at fairly low resolution thus far; jets in radio-strong quasars show polarized E vectors across the jet (inferring a projected magnetic field along the jet), while those in BLLac objects

show E vectors along the jet (inferring a projected B field across the jet). Superluminal motion is common in PSJ's, with $\beta_{app} \sim$ a few, and is always seen to be directed away from the (unresolved) core.

We find that both the emissivity and the apparent transverse velocity are very sensitive to the angle between the true velocity vector and the line of sight. This sensitivity means that the ballistic and wave models make quite different predictions for these observable quantities.

A. The Calculation

We consider a conical jet, of opening angle θ_{max} ; the line of sight makes an angle α with the jet axis. We work in Cartesian coordinates; \hat{x} and \hat{y} point across the jet; $\hat{z} = \hat{x} \times \hat{y}$ points along the jet axis. The line of sight, in this coordinate system, is

$$\hat{\mathbf{n}} = (-\sin \alpha, 0, \cos \alpha) \quad (9)$$

In polar coordinates, the jet can have a velocity field $\mathbf{v} = (v_r, 0, v_\phi)$ and a magnetic field $\tilde{\mathbf{B}} = (\tilde{B}_r, 0, \tilde{B}_\phi)$ (specified in the comoving frame). Converting to Cartesian coordinates and defining $v = \beta c$, we get

$$\begin{aligned} \mathbf{v} &= \left(v_\phi \frac{y}{R} + v_r \frac{x}{r}, v_\phi \frac{x}{R} + v_r \frac{y}{r}, v_r \frac{z}{r} \right) \\ &= c(\beta_x, \beta_y, \beta_z) \end{aligned} \quad (10a)$$

and

$$\begin{aligned} \mathbf{B} &= \left(\phi \frac{y}{R} + B_r \frac{x}{r}, B_\phi \frac{x}{R} + B_r \frac{y}{r}, B_r \frac{z}{r} \right) \\ &= (B_x, B_y, B_z) \end{aligned} \quad (10b)$$

if $R = (x^2 + y^2)^{1/2}$ and $r = (x^2 + y^2 + z^2)^{1/2}$.

We have written a numerical code to calculate the surface brightness (in total and polarized synchrotron emission) and also the emissivity-weighted apparent velocity, as a function of position across the jet. In order to simulate limb-brightened jets, we assume the radiating electrons only exist in the outer 10% of the jet, so that the emission is limited to the surface layer; other than this, we have not yet included any variation with jet radius. (The numerical code is fully general, however, and can handle inhomogeneous jets). We also choose an axisymmetric jet; however the results, discussed below, can easily be interpreted in terms of the observable signatures of a helical flow or wave pattern, as we will show.

To find the apparent velocity, we start with the general expression,

$$\mathbf{v}_{obs} = \frac{\hat{\mathbf{n}} \times (\mathbf{v} \times \hat{\mathbf{n}})}{(1 - \mathbf{v} \cdot \hat{\mathbf{n}}/c)} \quad (11)$$

and find the component which lies in the plane of the sky. After some algebra, we find the apparent velocity along the jet is,

$$\beta_{app,||} = \frac{\beta_x \cos \alpha + \beta_z \sin \alpha}{1 + \beta_x \sin \alpha - \beta_z \cos \alpha} \quad (12)$$

while that across the jet is,

$$\beta_{app,\perp} = \frac{\beta_y}{1 + \beta_x \sin \alpha - \beta_z \cos \alpha} \quad (13)$$

We calculate $\beta_{app,\parallel}$ and $\beta_{app,\perp}$ at each point along the sight, weighted by the local emissivity; integrating along the line of sight gives the observed transverse velocity.

To find the total and polarized emissivities, we need to evaluate the source functions for the Stokes I, Q and U parameters at each point along the line of sight. We first transform $\tilde{\mathbf{B}}$ to the observer's frame, \mathbf{B} (using standard Lorentz transforms), and express \mathbf{B} in Cartesian components. This gives, for the i th component,

$$B_i = \gamma \tilde{B}_i - (\gamma - 1) (\tilde{\mathbf{B}} \cdot \hat{\mathbf{v}}) \frac{\beta_i}{\beta} \quad (14)$$

if $\hat{\mathbf{v}}$ is a unit vector along \mathbf{v} . We then find the component of \mathbf{B} which lies in the plane of the sky,

$$\begin{aligned} \mathbf{B}_\perp &= \left[B_x + \sin \alpha (B_z \cos \alpha - B_x \sin \alpha), \right. \\ &\quad \left. B_y, B_z - \cos \alpha (B_z \cos \alpha - B_x \sin \alpha) \right] \\ &= (B_{\perp x}, B_{\perp y}, B_{\perp z}) \end{aligned} \quad (15)$$

Finally, we split \mathbf{B}_\perp into components along (B_Q) and across (B_U) the projected jet axis:

$$\begin{aligned} B_Q &= B_{\perp z} \cos \alpha + B_{\perp x} \sin \alpha \\ B_U &= B_{\perp y} \end{aligned} \quad (16)$$

From these, and using the Doppler factor

$$\delta = \frac{1}{\gamma(1 - \mathbf{v} \cdot \hat{\mathbf{n}}/c)} = \frac{1}{\gamma(1 - \beta_x \sin \alpha - \beta_z \cos \alpha)} \quad (17)$$

we get the source functions for the I, Q and U Stokes parameters:

$$\begin{aligned} S_I &= n_e B_\perp^{(s+1)/2} \delta^{(s+3)/2} \\ S_Q &= \pi S_I \frac{B_Q^2 - B_U^2}{B_\perp^2} \\ S_U &= \pi S_I \frac{B_Q B_U}{B_\perp^2} \end{aligned} \quad (18)$$

where $\pi = (s + 1)/(s + 7/3)$, and we have assumed the electron distribution function is a power law in energy, $n(E) \propto E^{-s}$.

B. Results

Using this code, we simulated the observables that would be seen in helical, ballistic trajectories and in helical waves propagating radially out along the jet. All runs reported here had $\beta = .998$, $\gamma = 15.8$, and a jet opening angle $\theta_{max} = 5^\circ$.

Helical, ballistic trajectories can be represented by an axisymmetric jet in which the velocity field has both v_r and v_ϕ components. We simulated cases with pitch angles ($\chi_v = \tan^{-1}(v_\phi/v_r)$) of 10° and 45° , with viewing angles α from 6° to 30° . These runs showed that helical trajectories *cannot* describe the data. Doppler boosting combined with the helical velocity component produces very strong limb brightening on one side (the approaching side) of the jet; *this as not seen in the data*. In addition, all runs for the $\chi_v = 45^\circ$ case and runs with $\alpha \lesssim 10^\circ$ for the $\chi_v = 10^\circ$ case show $\beta_{app} < 0$, meaning that features in the jet would appear to approach the core rather than move away from it. *This is also not seen in the data*. Thus, these simple models establish that the helical patterns seen in the PSJ are *not* due to true helical motion of luminous matter.

Helical waves can be represented by an axisymmetric jet in which the velocity field is radial ($v_\phi = 0$), but in which the magnetic field has both components. This would represent, for instance, a helical wave in which the field follows the perturbation. We simulated cases with magnetic field pitch angles $\chi_B = 20^\circ, 45^\circ$ and 75° . The surface brightness was found either to be limb brightened (at high viewing angles) or center brightened (at lower viewing angles), but within acceptable limits, and to be close to symmetric across the projected jet axis. The apparent velocities were always outward, again consistent with observations. Only the low magnetic pitch angles had E vectors across the jet (giving an inferred B field along the jet); higher χ_B models tended to have the inferred B across the jet. Thus, these models suggest that helical waves are consistent with PSJ observations, and further that the distinction between radio-strong quasars and BLLac objects may be as simple as the pitch angle of the jet magnetic field.

To summarize: we found that ballistic, helical motions *cannot* reproduce the observations. Relativistic aberration produces strong limb brightening on only one side of the jet; this is due to the asymmetries in the velocity field across the jet. *This is not seen in the data*. In addition, some combinations of helix pitch angle and line of sight angle lead to negative apparent velocities; the trajectories appear to *approach* the core. Again, this is not seen. Thus, we conclude that helical ballistic trajectories do not work.

Helical waves, on the other hand, do seem to work. Our simulations found the surface brightness to be either limb brightened, or center brightened (depending on helix and viewing angle), but within ranges consistent with the data. The apparent velocities are always outward, again consistent with observations. Varying the helix pitch angle can give either parallel or perpendicular projected B fields, possibly accounting for the QSR/BLL difference. Thus, these simulations strongly suggest that helical waves are the explanation of the observed structure in PSJ's.

III. WAVE MODES IN RELATIVISTIC PAIR JETS

We find that the helical PSJ features are very likely to be wave modes; they cannot be due to helical, ballistic motion. Thus, we need to understand what wave modes are possible in pair jets, and to determine their propagation speeds. In particular, we want to determine the relation of the possible modes, and their velocities, to the plasma density, internal energy, magnetic field, and streaming speed. While one would like to study the propagation (and stability) of general helical modes in a cylindrical or expanding jet, it is simpler to begin by considering waves in a uniform, homogenous medium. This has been our approach: to decouple the plasma-dependent results from results dependent on the specific geometry.

A. Low Frequency Modes in the PSJ Plasma

We started with the strongly magnetized limit: $B^2 \gg 8\pi u_e$, if $u_e = \int f(\beta)\gamma m_e c^2 d\beta$ is the internal energy density, due to a distribution function $f(\beta)$. In terms of fundamental frequencies, this is the limit $\omega_B \gg \omega_p$ (the cyclotron frequency much larger than the plasma frequency; both defined for a relativistic pair plasma). We considered a pair plasma moving at a bulk streaming speed (β_o, γ_o) . We also assumed the plasma is strongly anisotropic: $\beta_\perp \ll \beta_\parallel$. This situation is similar to that considered in pulsar polar caps, although the conditions in PSJs are probably less extreme. Thus, we can start with work already done for the pulsar situation. The waves most likely to be relevant to large-scale modes in PSJ's are transverse waves; the ones which become Alfvén or magnetosonic modes in cooler, everyday plasmas. To describe these waves in a cold, streaming plasma ($f(\beta) = f_o\delta(\beta - \beta_o)$), we use the dispersion relation given by Arons and Barnard (1986):

$$f(n) = (1 - n^2\mu^2) \left[(1 - \beta_o n\mu)^2 - R_p \right] - n^2(1 - \mu^2)(1 - \beta_o n\mu)^2 = 0 \quad (19)$$

Here, $n = ck/\omega$ is the index of refraction; $\mu = \cos\theta$ is the cosine of the propagation angle, and $R_p = \omega_p^2/\gamma_o^2\omega^2$ where ω_p is the cold plasma frequency: $\omega_p^2 = 4\pi ne^2/m_e$. This also describes waves in a warm, streaming plasma with a boxcar distribution, $f(\gamma) = f_o$ for $\beta_o < \beta < \beta_m$, if $\beta_m - \beta_o \ll \beta_o$ and $\gamma_o > 1$.

We find that this system has two low-frequency solutions ($R_p \gg 1$). We solve for $n_\parallel = n\mu$ (which gives the phase velocity), the group velocity (β_g, γ_g) , and the possibility of refraction (determined by comparing $v_{g,\perp}/v_{g,\parallel}$ to τ). One solution is the “slow mode”, with parallel index of refraction, dispersion relation and group velocity Lorentz factor,

$$\begin{aligned} n_\parallel &\simeq 1 + \frac{\tau^2}{8\gamma_o^4 R_p} \\ \omega &\simeq ck_\parallel \left(1 - \frac{\tau^2}{8\gamma_o^4 R_p} \right) \\ \gamma_g &\simeq \frac{4\gamma^2 R_p}{\tau} = \frac{4\omega_p^2}{\tau\gamma\omega^2} \end{aligned} \quad (20)$$

We have defined $\tau = \tan\theta$. This mode refracts: $v_{g,\perp}/v_{g,\parallel} \ll \tau$. Thus, it bends toward the field direction as it propagates. It has a near-lightlike relation between ω and k , as do Alfvénic waves in the strongly magnetized limit. In addition, $\gamma_g \gg \gamma_o$ for typical PSJ parameters: these waves will “run ahead” of the jet plasma, and give strong superluminal motion even in slow jets.

The second solution is the “very slow” mode, with

$$\begin{aligned} n_\parallel &\simeq \frac{R_p^{1/2}}{\beta_o(1 + \tau^2)^{1/2}} \\ \omega &\simeq ck_\parallel \frac{\beta_o(1 + \tau^2)^{1/2}}{R_p^{1/2}} \\ \gamma_g &\simeq \gamma \left(\frac{1 + \tau^2}{1 + \gamma^2\tau^2} \right)^{1/2} \end{aligned} \quad (21)$$

This mode has $v_{g,\perp}/v_{g,\parallel} \simeq \tau$; it is not refractive. It has k nearly independent of ω ; $k \simeq \omega_p/\gamma_o^{3/2} c$, to leading order (although it is also a transverse mode). It moves subrelativistically relative to the jet plasma; observed signal speeds from these waves will be essentially that of the underlying jet flow.

Thus, we find a very slow mode which essentially rides along with the streaming plasma (that is, its velocity relative to the comoving frame is subrelativistic). We also find a slightly slow mode, which propagates relativistically in the comoving frame; if this mode is related to the observed PSJ signals, their apparent transverse velocity *cannot* be identified with the streaming speed of the plasma.

B. Wave Modes in Pulsar Polar Caps, and Observational Tests

In the past year, we have extended this theory to describe waves at all possible frequencies in the pair plasma. We have also applied our theory to observational tests in the pulsar polar cap. Results from this work are in two preprints, Eilek (1996) and Eilek & Weatherall (1996).

We used our previous approach to find ordinary-mode solutions at all frequencies (Eilek 1996). That is, we found the modes in the comoving frame, where the dispersion relation is simple, and Lorentz-transformed them to the lab frame. This describes waves, as seen in the lab frame, propagating in a cold, relativistically streaming pair plasma; it is consistent with the results of Arons & Barnard (1986). The critical scaling frequency is ω_p , the local plasma frequency (we are still in the limit $\omega_p \ll \omega_B \rightarrow \infty$). We found that quite low frequencies, $\omega < \omega_p/\gamma^{3/2}$, are always subluminal, and also refractive; that is, their energy tends to flow along the local magnetic field. These low frequencies include the slightly slow mode, with parallel index of refraction $n_{\parallel} \simeq 1 + \tau^2 g \omega^2 / (8\omega_p^2)$, and the very slow mode, with $n_{\parallel} \simeq \omega_p / [\gamma^{3/2} \omega (1 + \tau^2)]$. These modes are likely to be the most relevant to large-scale PSJ features.

High frequencies, $\omega > \omega_p/\gamma^{3/2}$, however, can be either subluminal and refractive, or superluminal and not refractive. The difference depends on whether the frequency and propagation angle (relative to \mathbf{B}) in question transform to sub- or superluminal in the comoving frame. In addition, the index of refraction, $n = ck/\omega$, for frequencies $\omega > \omega_p/\gamma^{3/2}$ moving at small angles to \mathbf{B} shows an unusual frequency dependence. The common frequency dependence – for cold plasma in its rest frame, and for most mid-range and higher frequencies and most angles in the lab frame – is $|n - 1| \propto 1/\omega^2$. However, these mid-frequency, small-angle waves obey $|n - 1| \propto 1/\omega$; this leads to observable effects which may be used to test this theory.

How can such a calculation be tested? In this case, the question is, do these modes exist in pair plasmas, and if so are they the dominant ones? We propose using new-technology pulsar radio observations to answer this question, at least for pulsars. As stated above, the similarity of the pulsar and PSJ plasma environments make it reasonable to consider pulsars as another laboratory in which to test the microphysics of PSJ's. Both observational tests described below require high time resolution (~ 10 's of nsec), and an intrinsically narrow pulse in time. Pulsars satisfy the latter, and new technology allows the former; tests on pulsars may allow, by inference, conclusions to be drawn about PSJ's.

The flatter frequency dependence of n_{\parallel} for mid-range, low-angle modes makes such a test possible. We have calculated two easily observable quantities for these modes (Eilek 1996). The group velocity determines the dispersion measure – the dependence of pulse arrival time on frequency. The index of refraction itself determines the temporal broadening

of a signal, due to turbulent fluctuations in the signal path (Lee & Jokipii 1975). We find that both of these have different frequency dependences than produced by the usual cold, unmagnetized ISM plasma. In particular, the pulse arrival time changes with frequency as

$$\frac{dt_p(\omega)}{d\omega} \simeq \mp \frac{\tau^2}{4} \int_{r_{em}}^{R_{max}} \frac{\omega_{p\gamma}}{\omega^2} \frac{dr}{c} \quad (22)$$

and the pulse width obeys

$$t_D \simeq \frac{1}{32\pi^{5/2}} \frac{zD}{c} \frac{q_t^2}{q_o} \frac{\omega_p^2}{\gamma^3 \omega^2} \left(\frac{\delta n}{n} \right)^2 \quad (23)$$

Here, $\omega_{p\gamma} = \omega/\gamma^{3/2}$, D is the polar cap thickness, z is the distance to the pulsar, n is the pair plasma density, and q_t, q_o are the turbulent wavenumbers, perpendicular and parallel to \mathbf{B} . Both of these results show a flatter frequency dependence than the usual ISM signal (which has $dt_p/d\omega \propto 1/\omega^3$, and $t_D \propto 1/\omega^4$).

Thus, we predict both signals should be detectable from the pulsar polar cap, and in particular should be separable from ISM effects, due to their flatter frequency dependence. Detection of these effects will confirm that these modes are, indeed, important in the pulsar magnetospheric plasma. There is a further observational test possible. Pulsars show two types of emission region geometries: core pulsars have a filled, low-altitude cone of emission, while conal pulsars show emission only from the edges of a cone, and at somewhat higher altitudes (Rankin 1990). Pulsar polar cap theory, applied straightforwardly, predicts that only young pulsars should show strong pair cascades; these coincide surprisingly well with pulsars seen to have core emission. Conversely, conal pulsars are old ones, which the theory predicts should not have pair cascades. Since the amplitude of $dt_p/d\omega$ and t_D both depend on the pair density, we predict the relatively low density emission regions of conal pulsars should not show these effects (Weatherall & Eilek 1996).

C. Wave Modes in the PSJ Plasma: Finite Magnetic Field Effects

We next extended our analysis to include effects of a finite magnetic field. This of course complicates the system significantly. We again assumed a charge neutral pair plasma. In this work we retained terms in the inverse cyclotron frequency, and we also allowed relative streamings (parallel to the magnetic field, at $\beta_o = v_o/c$) between the electrons and the positrons (for instance, as would be induced by an electric field, and net current, in the jet).

We used standard plasma techniques to derive a general system of equations for the wave electric fields:

$$\begin{aligned} M_{xx}E_x + M_{xy}E_y + M_{xz}E_z &= 0 \\ M_{yx}E_x + M_{yy}E_y + M_{yz}E_z &= 0 \\ M_{zx}E_x + M_{zy}E_y + M_{zz}E_z &= 0 \end{aligned} \quad (24)$$

where the M_{ij} terms are standard components of the dispersion tensor. We note that this equation can be solved (in principle, when solutions exist) for the polarization (defined relative to the propagation direction, \mathbf{k})

$$\Pi_p = \frac{iE_a}{E_b} = i \cos \theta \left(\frac{E_x}{E_y} - \frac{E_z}{E_y} \tan \theta \right) \quad (25)$$

and that $\Pi_p \sim 1$ describes circular polarization, while $\Pi_p \ll 1$ or $\Pi_p \gg 1$ describe linear polarization. We evaluated the M_{ij} tensor for cold, streaming pair plasmas, in the limit $\omega, \omega_p \ll \Omega$ (strong but finite magnetic field), and found general dispersion solutions. We carried out the basic calculations in the comoving frame, and then transformed results to the observer's frame (assuming the plasma has a bulk velocity γ , for instance the flow speed of the jet.) We found that the comoving plasma frequency can be used to delineate solutions. We put primes on quantities measured in the comoving frame, and leave observer-frame quantities unprimed.

High Frequency, $\omega \gg \omega_p$ (comoving). In this limit, waves exist and propagate at all angles. We find that the waves are circularly polarized if (in the CMF)

$$\omega \gg \omega_p \quad \Rightarrow \quad \text{CP if} \quad \tau^2 \ll \frac{2\omega\beta_o}{\Omega_o} \quad (26)$$

Transformed to the lab frame, this describes the condition for circularly polarized waves:

$$\omega' \gg \omega'_p \quad \Rightarrow \quad \text{CP if} \quad \tau^2 \ll \frac{\omega}{\Omega_o} \frac{\Delta\gamma}{8\gamma^4} \quad (27)$$

Low Frequency, $\omega \ll \omega_p$ (comoving). In this limit, waves propagate only at small angles:

$$\tau^2 < -1 + r_p - 4\Delta^2 \left(1 - \frac{4\Delta^2}{r_p}\right) \quad (28)$$

and they are again significantly circularly polarized at small angles:

$$\omega \ll \omega_p \quad \Rightarrow \quad \text{CP if} \quad \tau^2 \ll \frac{4\omega_p^2\beta_o}{\omega\Omega_o} \quad (29)$$

Transforming this to the observer's frame, the condition for circular polarization is

$$\omega' \ll \omega'_p \quad \Rightarrow \quad \text{CP if} \quad \tau^2 \ll \frac{\omega_p^2}{\omega\Omega_o} \frac{\Delta\gamma}{\gamma^3} \quad (30)$$

We note that angles transform as $\tau \simeq \tau'/2\gamma$.

REFERENCES

- Arons, J. and Barnard, J. J., 1986, *Ap. J.*, 302, 120.
 Biretta, J. A., Owen, F. N. and Cornwell, T. J., 1989, *Ap. J.*, 342, 128.
 Cawthorne, T., 1991, in P. Hughes, ed, *Beams and Jets in Astrophysics*, 187.
 Eilek, J. A., 1996, submitted to *Ap. J.*
 Hughes, P. A., Aller, H. D. and Aller, M. F., 1985, *Ap. J.*, 298, 301.
 Konigl, A., 1981, *Ap. J.*, 243, 700.
 Lee, L. C. & Jokipii, J. R., 1975, *Ap. J.*, 196, 695; 201, 532.
 Lovelace, R. V. E., Wang, J. C. L. & Sulkanen, M. E., 1987, *Ap. J.*, 315, 504.

- Marscher, A. P. and Gear, W. K., 1985, *Ap. J.*, 298, 114.
- Rankin, J., 1990, *Ap. J.*, 352, 247.
- Readhead, A. C. S., Venturi, T., Marr, J. M. and Backer, D. C., 1990, in Zensus and Pearson, *op cit.*
- Wang, J. C. L., Sulkanen, M. E. & Lovelace, R. V. E., 1990, *Ap. J.*, 355, 38.
- Weatherall, J. and Eilek, J. A., 1996, *Ap. J.*, xx, yy.
- Wilkinson, P. N., Tzioumis, A. K., Akojur, C. E., Benson, J. M., Walker, R. C. and Simon, R. S., 1990, in Zensus and Pearson, *op cit.*